

# Robust states in semiconductor quantum dot molecules

H. S. Borges, L. Sanz, J. M. Villas-Bôas and A. M. Alcalde

*Instituto de Física, Universidade Federal de Uberlândia, 38400-902, Uberlândia-MG, Brazil*

Semiconductor quantum dots coherently driven by pulsed laser are fundamental physical systems which allow studying the dynamical properties of confined quantum states. These systems are attractive candidates for a solid-state qubit, which open the possibility for several investigations in quantum information processing. In this work we study the effects of a specific decoherence process, the spontaneous emission of excitonic states, in a quantum dot molecule. We model our system considering a three-level Hamiltonian and solve the corresponding master equation in the Lindblad form. Our results show that the spontaneous emission associated with the direct exciton helps to build up a robust indirect exciton state. This robustness against decoherence allows potential applications in quantum memories and quantum gate architectures. We further investigate several regimes of physical parameters, showing that this process is easily controlled by tuning of external fields.

PACS numbers: 73.21.La, 73.40.Gk, 03.65.Yz

## I. INTRODUCTION

The advance on the manipulation and dynamical control of quantum states under the action of coherent radiation has recently become a subject of intense research in condensed matter physics. Dynamical control is a necessary step for the implementation of any protocol associated with Quantum Information Processing (QIP) [1]. In this sense, semiconductor quantum dots (QDs) has been proved to be an ideal candidate. Using strong resonant laser pulses and different probe techniques, several different groups have successfully demonstrated coherent manipulation of the exciton population of a single QD. [2–7] They demonstrated a process known as Rabi oscillation which is indeed a proof of the exciton qubit rotation. Unlike atoms, however, QDs suffer from unavoidable variation in their size, and the presence of a surrounding environment with which they may interact strongly, making the entire system to lose its phase quickly [8–10]. The main interest in QDs arises from their characteristic discrete energy spectrum, and its great flexibility in change it, not only by manipulation of their geometric structure, but also with the application of external gates. A natural next step for the development of such system is to put two quantum dots together and allowing them to couple. A lot of work has been done in this direction, where beautiful examples of a molecule formation have been achieved [11–22]. However, the coherent dynamics of such objects under strong laser pumping remains largely unexplored experimentally, and our work can give further insight to help the experimental development.

In this paper, we study the effects of the spontaneous decay in the excitonic states of a self-assembled semiconductor quantum dot molecule (QDM) coupled by tunneling and under the influence of an external electromagnetic field. We use a standard density matrix approach in the Lindblad form to describe the system dynamics and our results indicate that the spontaneous decay of the direct exciton helps to build up a coherent population of the indirect exciton (electron and hole in different dots),

which has a longer lifetime due to its spatial separation with small overlap of the wave function. This effect is robust to the changes of external parameters and in order to describe it we describe the physical system and the detailed theoretical model in Sec. II, then in Sec. III we show the results of numerical calculations, followed by our conclusions in Sec. IV.

## II. THEORY AND MODEL

The physical system we consider here is an asymmetric double quantum dot coupled by tunneling. Electrons and holes can be confined in either dot and we can use a near-resonant optical pulse to promote electrons from the valence to the conduction band, creating an electron-hole correlated state known as exciton. Electrons or holes can then tunnel to the other dot, creating an indirect exciton. An external electric field, applied in the growth direction, brings the individual levels of electrons or holes into resonance, favoring the tunneling. Nevertheless, in asymmetric QDM structures it is even possible to control which type of carrier, electron or holes, tunnels [23]. In this situation, we can safely neglect the tunneling of holes as the electric field brings one level (conduction band) more into resonance while makes the other (valence band) more out of resonance. With this assumption, the dynamics of the QDM can be modeled by a simple three-level system, where the ground state  $|0\rangle$  is a molecule without any excitation,  $|1\rangle$  is the system with one exciton in the left dot, while  $|2\rangle$  is the system with one indirect exciton, after the electron has tunneled. The schematic configuration of levels and physical parameters are shown in the Fig. 1, where we also include the decoherence channels associated with spontaneous emission of excitonic states ( $\Gamma_0^1, \Gamma_0^2$ ).

Using the rotating wave approximation and dipole ap-

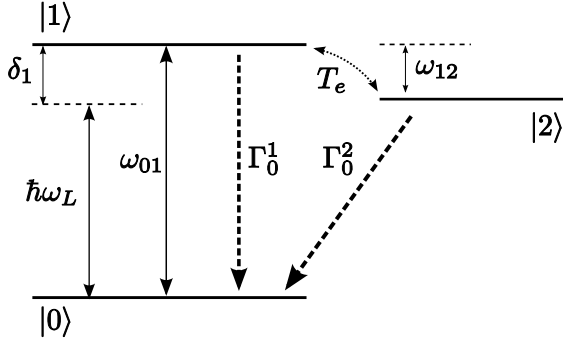


FIG. 1: Scheme of energy levels with physical parameters on Hamiltonian (1).

proximation, the system Hamiltonian is written as [24]:

$$\hat{H}(t) = \sum_{j=0}^2 \hbar\omega_j |j\rangle\langle j| + T_e(|1\rangle\langle 2| + |2\rangle\langle 1|) + \hbar\Omega(e^{i\omega_L t}|0\rangle\langle 1| + e^{-i\omega_L t}|1\rangle\langle 0|), \quad (1)$$

where  $\omega_j$  are the frequencies of  $|j\rangle$ -th states ( $j = 0, 1, 2$ ),  $T_e$  is the tunneling coupling,  $\omega_L$  is the frequency of the applied laser and the dipole coupling is  $\Omega = \langle 0|\vec{\mu} \cdot \vec{E}|1\rangle/2\hbar$ , where  $\vec{\mu}$  is the electric dipole moment and  $\vec{E}$  is the amplitude of incident field. The intensity of incident field can be easily controlled to provide available conditions for the coherent control of the system quantum state. We also assume a low-intensity incident pulse, so the Rabi frequency is significantly smaller than the intraband excitation energy [25],  $\Omega \ll \omega_{10} = \omega_1 - \omega_0$  and  $\omega \approx \omega_{10}$ . Under this assumption, we might consider that only the ground-state exciton can be formed in our system.

Applying the unitary transformation [24]

$$\hat{U} = \exp\left[\frac{i\omega_L t}{2}(|1\rangle\langle 1| - |0\rangle\langle 0| + |2\rangle\langle 2|)\right], \quad (2)$$

and using the *Baker-Hausdorff lemma* [26], we obtain a time-independent version of Hamiltonian (1) written as follows:

$$\hat{H}' = \frac{1}{2} \begin{pmatrix} -\delta_1 & 2\hbar\Omega & 0 \\ 2\hbar\Omega & \delta_1 & 2T_e \\ 0 & 2T_e & \delta_2 \end{pmatrix}, \quad (3)$$

where  $\delta_1 = \hbar(\omega_{10} - \omega_L)$  is the detuning between the frequency of optical pulse and exciton transition,  $\delta_2 = \delta_1 + 2\hbar\omega_{21}$  and  $\omega_{ij}$  is the optical transition between  $i$  and  $j$  energy states.

To taking into account the effects of decoherence, we used the Liouville-Von Neumann-Lindblad equation given by [27]:

$$\frac{\partial \hat{\rho}(t)}{\partial t} = -\frac{i}{\hbar}[\hat{H}', \hat{\rho}(t)] + \hat{L}(\hat{\rho}(t)). \quad (4)$$

Here,  $\hat{\rho}(t)$  is the density matrix operator. The Liouville operator,  $\hat{L}(\hat{\rho})$ , describes the dissipative process. Assuming the Markovian approximation, Liouville operator can be written as [28]:

$$\hat{L}(\hat{\rho}) = \frac{1}{2} \sum_i \Gamma_j^i (2|j\rangle\langle i|\hat{\rho}|i\rangle\langle j| - \hat{\rho}|i\rangle\langle i| - |i\rangle\langle i|\hat{\rho}), \quad (5)$$

where  $\Gamma_j^i$  corresponds to the decoherence rates due spontaneous decay from the state  $|i\rangle$  to the state  $|j\rangle$ . In order to investigate the dynamics associated with this physical system, we solve the master equation (4), and found the density matrix coefficients at certain time  $t$ . Writing Eq.(4) in the basis defined by  $|0\rangle$ ,  $|1\rangle$  and  $|2\rangle$  states, we obtain a set of nine coupled linear differential equations written as:

$$\begin{aligned} \dot{\rho}_{00} &= -i\Omega(\rho_{10} - \rho_{01}) + \Gamma_0^1\rho_{11} + \Gamma_0^2\rho_{22}, \\ \dot{\rho}_{01} &= \frac{i}{\hbar} [\delta_1\rho_{01} + \hbar\Omega(\rho_{00} - \rho_{11}) + T_e\rho_{02}] - \frac{1}{2}\Gamma_0^1\rho_{01}, \\ \dot{\rho}_{02} &= \frac{i}{\hbar} \left[ \frac{\rho_{02}}{2}(\delta_1 + \delta_2) - \hbar\Omega\rho_{12} + T_e\rho_{01} \right] - \frac{1}{2}\Gamma_0^2\rho_{02}, \\ \dot{\rho}_{10} &= \frac{i}{\hbar} [-\delta_1\rho_{10} + \hbar\Omega(\rho_{11} - \rho_{00}) - T_e\rho_{20}] - \frac{1}{2}\Gamma_0^1\rho_{10}, \\ \dot{\rho}_{11} &= \frac{i}{\hbar} [\hbar\Omega(\rho_{10} - \rho_{01}) + T_e(\rho_{12} - \rho_{21})] - \Gamma_0^1\rho_{11}, \\ \dot{\rho}_{12} &= \frac{i}{\hbar} \left[ \frac{\rho_{12}}{2}(\delta_2 - \delta_1) - \hbar\Omega\rho_{02} + T_e(\rho_{11} - \rho_{22}) \right] \\ &\quad - \frac{1}{2}(\Gamma_0^1 + \Gamma_0^2)\rho_{12}, \\ \dot{\rho}_{20} &= \frac{i}{\hbar} \left[ -\frac{\rho_{20}}{2}(\delta_2 + \delta_1) + \hbar\Omega\rho_{21} - T_e\rho_{10} \right] - \frac{1}{2}\Gamma_0^2\rho_{20}, \\ \dot{\rho}_{21} &= \frac{i}{\hbar} \left[ \frac{\rho_{21}}{2}(\delta_1 - \delta_2) + \hbar\Omega\rho_{20} + T_e(\rho_{22} - \rho_{11}) \right] \\ &\quad - \frac{1}{2}(\Gamma_0^1 + \Gamma_0^2)\rho_{21}, \\ \dot{\rho}_{22} &= \frac{i}{\hbar} T_e(\rho_{21} - \rho_{12}) - \Gamma_0^2\rho_{22}. \end{aligned} \quad (6)$$

In order to solve the set of equations (6), we rewrite as  $\dot{\rho} = A\rho$ , considering  $\rho$  as a column vector and  $A$  being a square matrix associated with the coefficients of the coupled system above. The solution can be written as

$$\rho_{ij}(t) = \sum_{j=0}^8 S_{ij} e^{\lambda_j t} (S_{ij}^{-1} \rho_{ij}(0)), \quad (7)$$

where,  $\lambda_j$  and  $S_{ij}$  are the eigenvalues and the matrix formed by the eigenvectors of matrix  $A$ , respectively.  $\rho_{ij}(0)$  are the elements of the density matrix operator at  $t = 0$ .

### III. RESULTS AND DISCUSSION

For our calculations, we consider the following values of physical parameters:  $\hbar\omega_{10} \simeq 1.6$  eV [3, 29],

$\Omega \simeq 0.05 - 1.0$  meV [25, 30],  $\Gamma_0^1 \simeq 0.33 - 6.6$   $\mu\text{eV}$  [30, 31], and  $\Gamma_0^2 \simeq 10^{-4}\Gamma_0^1$  [32]. The tunneling coupling, which depends the barrier characteristics and the external electric field, was selected as:  $T_e \simeq 0.01 - 0.1$  meV [33] or  $T_e \simeq 1 - 10$  meV [34], for weak and strong tunneling regime, respectively. The system dynamics depends also from the detunings  $\delta_1$  and  $\delta_2$ . Experimentally,  $\delta_1$  is controlled by varying the frequency of external laser. The value of  $\delta_2$  is changed by varying  $\delta_1$  and the frequency transition  $\omega_{21}$ , which can be done by manipulation of external electric field that changes the effective confinement potential. By varying this set of parameters we are able to perform a coherent manipulation of the wave function of the system. For all simulations, we consider  $|\Psi(0)\rangle = |0\rangle$  as initial condition.

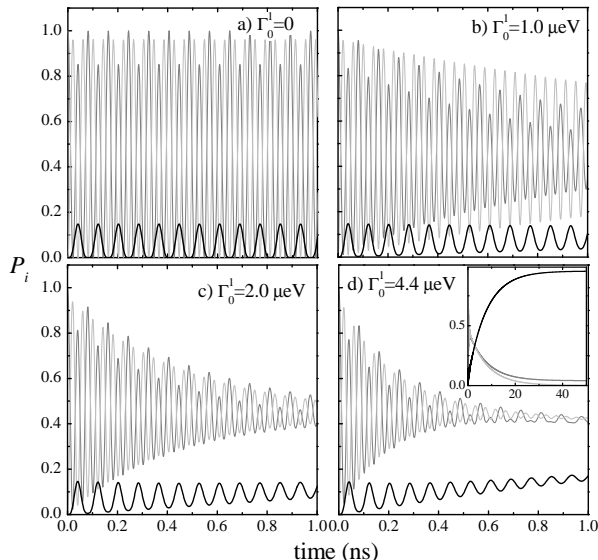


FIG. 2: Dynamics of populations,  $P_i$ , of level  $|i\rangle$  ( $i = 0, 1, 2$ ) as function of time for different choices of spontaneous emission rate  $\Gamma_0^1$  with parameters  $\delta_1 = 0$ ,  $\omega_{21} = 0$ ,  $\Omega = 50$   $\mu\text{eV}$  and  $T_e = 10$   $\mu\text{eV}$ . We use gray line for  $P_0$ , light-gray line for  $P_1$  and black line for  $P_2$ . (a) Non-dissipative dynamics ( $\Gamma_0^1 = 0$ ); (b)  $\Gamma_0^1 = 1.0$   $\mu\text{eV}$ ; (c)  $\Gamma_0^1 = 2.0$   $\mu\text{eV}$ ; (d)  $\Gamma_0^1 = 4.4$   $\mu\text{eV}$ .

Our first task is to analyze the effect on population dynamics of the decoherence process associated with spontaneous emission of direct exciton. In Fig. 2, we plot the probability of occupation associated with each of the three levels considering different values of spontaneous emission rate  $\Gamma_0^1$ . For the physical parameters considered here, the non-dissipative dynamics ( $\Gamma_0^1 = 0$ ) shows that there are Rabi oscillations between the three levels of the system. This is illustrated in Fig. 2 a). The population of indirect exciton, state  $|2\rangle$ , depends directly on the parameter  $T_e$ , although the value of the coupling  $\Omega$  and detunings  $\delta_1$  and  $\omega_{21}$ , has important effects on dynamics [24]. The situation changes when spontaneous emission is taken into account. As we expected, the Rabi oscillations become damped. This can be seen in Figs. 2 b), c) and d). For long times and values of  $\Gamma_0^1$  high enough,

as shown in the inset of Fig. 2 d), the Rabi oscillations are suppressed and the electron wave function tends to an asymptotic state.

Now we focus our attention on the formation of a stationary state with high population of indirect excitonic level,  $|2\rangle$ . With a lifetime significantly longer (about  $10^4$  times the direct exciton) [32], this particular state shows more potential for quantum information processing than the direct exciton,  $|1\rangle$  state. In order to study the effects of several physical parameters on Hamiltonian (1) and the decoherence, we study the behavior of average occupation of state  $|2\rangle$ , defined as

$$\overline{P_2} = \frac{1}{t_\infty} \int_0^{t_\infty} P_2(t) dt.$$

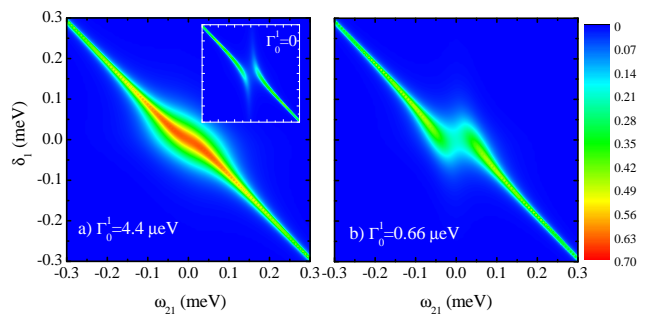


FIG. 3: (Color online) Average population of state  $|2\rangle$ ,  $\overline{P_2}$ , as function of detuning,  $\delta_1$  and frequency  $\omega_{21}$  for  $\Omega = 50$   $\mu\text{eV}$ ,  $T_e = 10$   $\mu\text{eV}$  and  $\Gamma_0^2 \approx 10^{-4}\Gamma_0^1$ . a)  $\Gamma_0^1 = 4.4$   $\mu\text{eV}$ . Inset:  $\overline{P_2}$  for  $\Gamma_0^1 = 0$  and the same values of  $\Omega$  and  $T_e$ . b)  $\Gamma_0^1 = 0.66$   $\mu\text{eV}$ .

In Fig. 3, we plot our results for  $\overline{P_2}$ , as function of laser detuning  $\delta_1$  and frequency  $\omega_{21}$ , considering two different values of the direct exciton spontaneous emission rate,  $\Gamma_0^1$ . Bright colors are associated with high values of  $\overline{P_2}$ , which means an efficient transference of the electron from the first to the second dot. From our results, it is possible to conclude that a large occupation probability of  $|2\rangle$  is obtained if the detuning  $\delta_1$  is balanced with the applied electric field so that  $\delta_1 + \omega_{21} \simeq 0$ . We will name this condition as *balanced detuning*. The behavior considering full resonance between the three levels ( $\delta_1 \simeq \omega_{21} \simeq 0$ ) deserves more attention. Let us define an area associated with the full resonance condition  $|\delta_1|, |\omega_{21}| \lesssim 50 \mu\text{eV}$ : when spontaneous emission is not considered ( $\Gamma_0^1 = 0$ ), the average population  $\overline{P_2}$  is near to zero, as shown in Ref. [24] and in the inset of Fig. 3 a). Thus, full resonance condition is not a good experimental choice for an optimal creation of indirect excitonic state. Considering the effects of spontaneous emission  $\Gamma_0^1$ , we can observe a different behavior: the values of  $\overline{P_2}$  at point  $(\omega_{21}, \delta_1) = (0, 0)$  increase from 0.05 (for  $\Gamma_0^1 = 0$ ) to  $\simeq 0.6$  (for  $\Gamma_0^1 = 4.4$   $\mu\text{eV}$ ) and  $\simeq 0.2$  (for  $\Gamma_0^1 = 0.66$   $\mu\text{eV}$ ). This shows that for realistic direct excitons, with a non-zero spontaneous emission rate, the transfer of the electron between dots is more efficient.

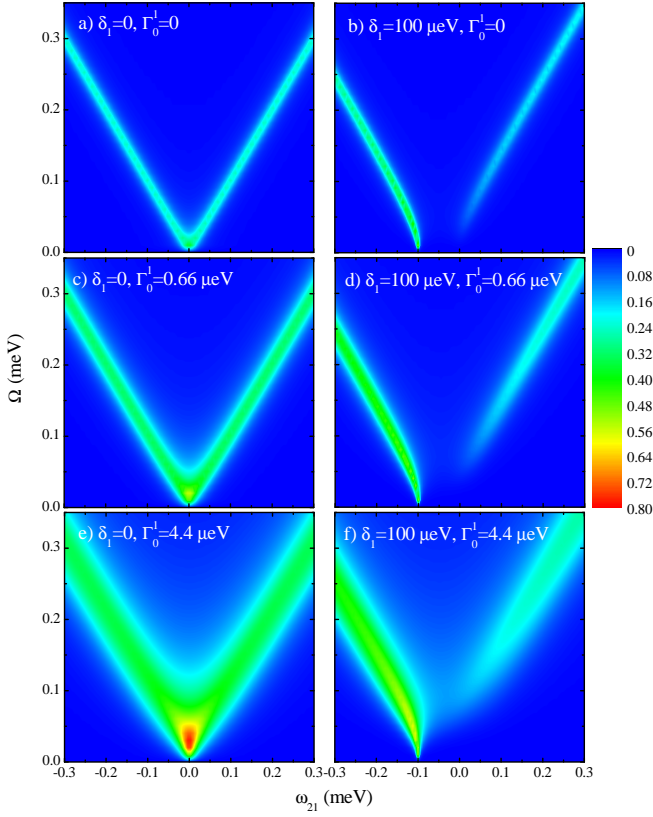


FIG. 4: (Color online). Average population of state  $|2\rangle$ ,  $\overline{P}_2$ , as function of coupling parameter  $\Omega$ , and frequency  $\omega_{21}$  for resonant and non-resonant condition. a)  $\Gamma_0^1 = 0$  and  $\delta_1 = 0$ ; b)  $\Gamma_0^1 = 0$  and  $\delta_1 = 100 \mu\text{eV}$ ; c)  $\Gamma_0^1 = 0.66 \mu\text{eV}$  and  $\delta_1 = 0$ ; d)  $\Gamma_0^1 = 0.66 \mu\text{eV}$  and  $\delta_1 = 100 \mu\text{eV}$ ; e)  $\Gamma_0^1 = 4.4 \mu\text{eV}$  and  $\delta_1 = 0$ ; f)  $\Gamma_0^1 = 4.4 \mu\text{eV}$  and  $\delta_1 = 100 \mu\text{eV}$ . In all cases,  $T_e = 10 \mu\text{eV}$  and  $\Gamma_0^2 \approx 10^{-4}\Gamma_0^1$

In Fig. 4, we show our results for average population,  $\overline{P}_2$ , as a function of both, frequency  $\omega_{21}$  and dipole coupling  $\Omega$ , for different choices of  $\Gamma_0^1$  considering  $\delta_1 = 0$ , Figs. 4 a), c) and e), and  $\delta_1 = 100 \mu\text{eV}$ , Figs. 4 b), d) and f). For all cases, we are able to populate the indirect exciton state, evidenced by bright regions with values of  $\overline{P}_2$  larger than 0.3. At resonance condition, Figs. 4 a), c) and e), this bright area have a V-like form, with higher values of  $\overline{P}_2$  concentrated on a small area associated with low values of  $\Omega$  and  $\omega_{21}$ . For non-resonant condition, the symmetry between negative and positive values of  $\omega_{21}$  is broken. Still, the large values of  $\overline{P}_2$  are obtained when the condition  $\delta_1 + \omega_{21} \simeq 0$  is fulfilled. The action of spontaneous emission can be analyzed by comparing the different situations shown in Fig. 4. Higher values of parameter  $\Gamma_0^1$  are connected with higher values of average population  $\overline{P}_2$ . For example, in Fig. 4 a) when  $\Gamma_0^1 = 0$  the maximum value of  $\overline{P}_2 \simeq 0.36$ . Considering decoherence, the maximum value of  $\overline{P}_2$  goes from 0.6 for  $\Gamma_0^1 = 0.66 \mu\text{eV}$  [Fig. 4 c)] to  $\simeq 0.8$  for  $\Gamma_0^1 = 4.4 \mu\text{eV}$  [Fig. 4 d)]. Also, the total area for highly efficient population of  $|2\rangle$  state in-

crease as spontaneous emission increase: both, the arms of the characteristic V area and the region with best values of  $\overline{P}_2$  become progressively large when the value of  $\Gamma_0^1$  increase.

It is useful to check the combined effect of both, the tunneling and decoherence. It is expected a good transfer of population associated with higher values of  $T_e$  parameter. This can be verified by comparing the results  $\overline{P}_2$  without the effect of decoherence process with  $T_e = 10 \mu\text{eV}$ , Fig. 4 a), with the results considering a higher value of tunneling parameter  $T_e = 50 \mu\text{eV}$ , Fig. 5 a). The effect of decoherence process is illustrated by Fig. 5 b). Notice that area on Fig. 5 with high  $\overline{P}_2$  increase by the action of decoherence and the maximum value of  $\overline{P}_2$  goes from  $\simeq 0.4$ , in Fig. 5 a), to  $\overline{P}_2 \simeq 0.8$  in Fig. 5 b).

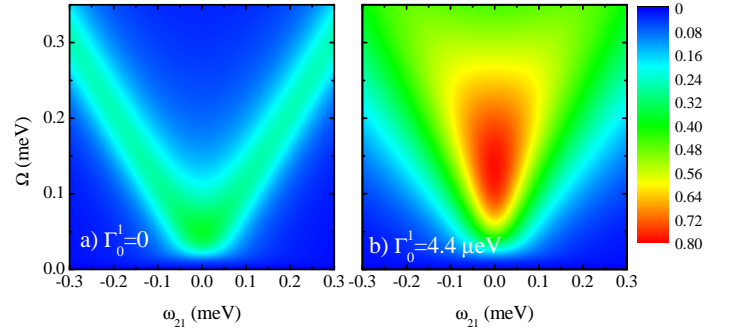


FIG. 5: (Color online). Average occupation of state  $|2\rangle$ ,  $\overline{P}_2$ , as function of coupling parameter,  $\Omega$ , and frequency  $\omega_{21}$  considering  $T_e = 50 \mu\text{eV}$ ,  $\delta_1 = 0$  and  $\Gamma_0^2 \approx 10^{-4}\Gamma_0^1$ . (a)  $\Gamma_0^1 = 0$ . (b)  $\Gamma_0^1 = 4.4 \mu\text{eV}$ .

After our analysis of  $\overline{P}_2$ , it is necessary to check the actual behavior of level population  $P_2$ . In Fig. 6, we plot  $P_2$  considering some choices of physical parameters associated with our previous analysis (Figs. 2 - 5). In all cases, we limit ourselves to full resonance condition ( $\delta_1 \simeq \omega_{21} \simeq 0$ ). When dynamics is associated with stationary states, the value of  $\overline{P}_2$  depends on two aspects: the final value of  $P_2$  at stationary state and the time needed to reach this maximum value. In Fig. 6 a) we plot  $P_2$  for  $\Omega = 50 \mu\text{eV}$  and  $T_e = 10 \mu\text{eV}$  considering different values of  $\Gamma_0^1$ . We can conclude that a higher spontaneous emission rate of the direct exciton is connected with a faster evolution to the asymptotic value of  $P_2$ . That means, the broadening effects (short lifetime) on the direct exciton are advantageous if we are interested on manipulate electronic wave function in order to create an asymptotic state with high values of  $P_2$  at short times.

Next, we verify that the exact maximum value of  $P_2$  is related with coupling parameters  $\Omega$  and  $T_e$  and, also, with the balanced detuning condition  $\delta_1 + \omega_{21} \simeq 0$ . From our calculations of average occupation of indirect excitonic state, we analyse the behavior of  $P_2$  considering a set of  $\Omega$  and  $T_e$  parameters associated with maximum values of  $\overline{P}_2$  for two different  $\Gamma_0^1$  rates.

The evolution of population  $P_2$  is shown in Fig. 6 b),

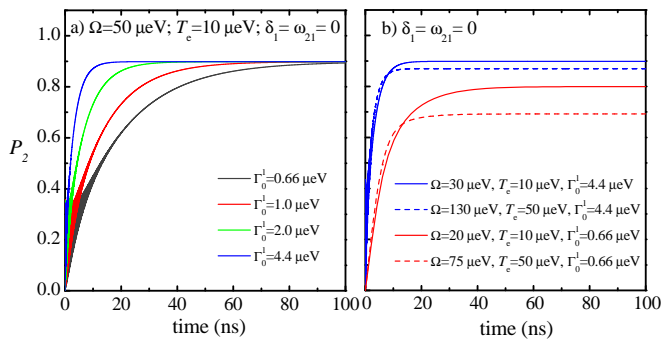


FIG. 6: (Color online) Population of indirect exciton state,  $P_2$ , as function of time at stationary regime. (a)  $P_2$  for different values of spontaneous emission rate  $\Gamma_0^1$  considering full resonance condition ( $\delta_1 = 0$ ,  $\omega_{21} = 0$ ) for coupling parameters  $\Omega=50 \mu\text{eV}$  and  $T_e=10 \mu\text{eV}$ . (b)  $P_2$  associated with the physical parameters for the highest values of  $\overline{P_2}$  founded in Fig.4 and Fig.5.

blue (red) lines represent the  $\Gamma_0^1=4.4 \mu\text{eV}$  ( $\Gamma_0^1=0.66 \mu\text{eV}$ ) situation. For a fixed value of  $\Gamma_0^1$ , we can define the characteristic time  $t_0$  as the time at which the system reaches the asymptotic value of  $P_2$  (for example  $t_0 \simeq 14\text{ns}$  for  $\Gamma_0^1 = 0.66 \mu\text{eV}$ ). This characteristic time, which depends on the value of  $\Gamma_0^1$ , allows us to distinguish two dynamical regimes: 1) for long time,  $t \gg t_0$  the population is essentially independent of time and its maximum value depends directly on the  $\Omega/T_e$  rate value (the population increases when this rate increases). 2) at short times,  $t < t_0$ , the dynamics does not depend on the value of  $\Omega/T_e$ , being governed mainly by  $\Gamma_0^1$ . Comparing all cases plotted in Fig. 6 b) we can conclude that the condition to obtain an asymptotic state with large values of the occupation  $P_2$ , associated with short characteristic times  $t_0$ , is given by  $\frac{\Omega}{T_e} \simeq \frac{T_e}{\Gamma_0^1}$ . Thus, it is possible to obtain experimentally optimized values of  $P_2$ , by adjusting appropriately the laser intensity  $\Omega$  for fixed values of  $T_e$  and  $\Gamma_0^1$ , which in turn can be obtained through optical

spectroscopy.

#### IV. SUMMARY

In this work, we use a standard density matrix approach in the Lindblad form to model the dynamics of a Quantum Dot Molecule under the influences of external electric and electromagnetic fields, and in the presence of spontaneous emission. By numerically solving the density matrix we show that the spontaneous decay of the direct exciton helps to build up a coherent population of the indirect exciton, which should have important applications in quantum information processing due to its longer coherence time.

We further investigate the efficiency of creation of indirect exciton state as function of physical parameters of our model. For weak spontaneous emission rate, the system presents a Rabi oscillation and in the opposite limit the system rapidly build up a stationary population of the indirect exciton. Our results shown that the population of the indirect exciton is strongly influenced by the spontaneous emission of the direct exciton. We demonstrate that the indirect exciton, which has a longer lifetime, is robust against the spontaneous emission process. Finally, at maximum average population conditions, we determined a relation between the relevant parameters of the system which allows us to obtain large populations of indirect exciton  $P_2 \simeq 0.9$ .

#### Acknowledgments

The authors gratefully acknowledge financial support from Brazilian Agencies CAPES, CNPq and FAPEMIG. This work was performed as part of the Brazilian National Institute of Science and Technology for Quantum Information (INCT-IQ).

- 
- [1] D. P. DiVincenzo, Fortschritte der Physik **48**, 771 (2000).
  - [2] T. H. Stievater, X. Li, D. G. Steel, D. Gammon, D. S. Katzer, D. Park, C. Piermarocchi, and L. J. Sham, Phys. Rev. Lett. **87**, 133603 (2001).
  - [3] H. Kamada, H. Gotoh, J. Temmyo, T. Takagahara, and H. Ando, Phys. Rev. Lett. **87**, 246401 (2001).
  - [4] H. Htoon, T. Takagahara, D. Kulik, O. Baklenov, J. A. L. Holmes, and C. K. Shih, Phys. Rev. Lett. **88**, 087401 (2002).
  - [5] A. Zrenner, E. Beham, S. Stuffer, F. Findeis, M. Bichler, and G. Abstreiter, Nature **418**, 612 (2002).
  - [6] Q. Q. Wang, A. Muller, P. Bianucci, E. Rossi, Q. K. Xue, T. Takagahara, C. Piermarocchi, A. H. MacDonald, and C. K. Shih, Phys. Rev. B **72**, 035306 (2005).
  - [7] S. Stuffer, P. Ester, A. Zrenner, and M. Bichler, Phys. Rev. B **72**, 121301 (2005).
  - [8] A. Vasanelli, R. Ferreira, and G. Bastard, Phys. Rev. Lett. **89**, 216804 (2002).
  - [9] J. Forstner, C. Weber, J. Danckwerts, and A. Knorr, Phys. Rev. Lett. **91**, 127401 (2003).
  - [10] J. M. Villas-Boas, S. E. Ulloa, and A. O. Govorov, Phys. Rev. Lett. **94**, 057404 (2005).
  - [11] M. Bayer, P. Hawrylak, K. Hinzer, S. Fafard, M. Korkusinski, Z. R. Wasilewski, O. Stern, and A. Forchel, Science **291**, 451 (2001).
  - [12] P. Borri, W. Langbein, U. Woggon, M. Schwab, M. Bayer, S. Fafard, Z. Wasilewski, and P. Hawrylak, Phys. Rev. Lett. **91**, 267401 (2003).
  - [13] V. G. Talalaev, J. W. Tomm, N. D. Zakharov, P. Werner, B. V. Novikov, and A. A. Tonkikh, Appl. Phys. Lett. **85**, 284 (2004).
  - [14] M. Rontani, S. Amaha, K. Muraki, F. Manghi, E. Moli-

- nari, S. Tarucha, and D. G. Austing, *Phys. Rev. B* **69**, 085327 (2004).
- [15] H. J. Krenner, M. Sabathil, E. C. Clark, A. Kress, D. Schuh, M. Bichler, G. Abstreiter, and J. J. Finley, *Phys. Rev. Lett.* **94**, 057402 (2005).
- [16] E. T. Batteh, J. Cheng, G. Chen, D. G. Steel, D. Gammon, D. S. Katzer, and D. Park, *Phys. Rev. B* **71**, 155327 (2005).
- [17] C. Bardot, M. Schwab, M. Bayer, S. Fafard, Z. Wasilewski, and P. Hawrylak, *Phys. Rev. B* **72**, 035314 (2005).
- [18] G. Ortner, I. Yugova, G. B. H. von Hogersthal, A. Larionov, H. Kurtze, D. R. Yakovlev, M. Bayer, S. Fafard, Z. Wasilewski, P. Hawrylak, et al., *Phys. Rev. B* **71**, 125335 (2005).
- [19] H. J. Krenner, S. Stuffer, M. Sabathil, E. C. Clark, P. Ester, M. Bichler, G. Abstreiter, J. J. Finley, and A. Zrenner, *New Journal of Physics* **7**, 184 (2005).
- [20] T. Unold, K. Mueller, C. Lienau, T. Elsaesser, and A. D. Wieck, *Phys. Rev. Lett.* **94**, 137404 (2005).
- [21] E. A. Stinaff, M. Scheibner, A. S. Bracker, I. V. Ponomarev, V. L. Korenev, M. E. Ware, M. F. Doty, T. L. Reinecke, and D. Gammon, *Science* **311**, 636 (2006).
- [22] L. Robledo, J. Elzerman, G. Jundt, M. Atature, A. Hoge, S. Falt, and A. Imamoglu, *Science* **320**, 772 (2008).
- [23] A. S. Bracker, M. Scheibner, M. F. Doty, E. A. Stinaff, I. V. Ponomarev, J. C. Kim, L. J. Whitman, T. L. Reinecke, and D. Gammon, *Appl. Phys. Lett.* **89**, 233110 (2006).
- [24] J. Villas-Bôas, A. Gororov, and S. Ulloa, *Phys. Rev. B* **69**, 125342 (2004).
- [25] T. Calarco, A. Datta, P. Fedichev, E. Pazy, and P. Zoller, *Phys. Rev. A* **68**, 012310 (2003).
- [26] J. J. Sakurai, *Modern Quantum Mechanics* (Addison Wesley, 1994).
- [27] A. R. P. Rau and W. Zhao, *Phys. Rev. A* **68**, 052102 (2003).
- [28] J. Villas-Bôas, S. Ulloa, and A. Gororov, *Phys. Rev. B* **75**, 155334 (2007).
- [29] N. H. Bonadeo, J. Erland, D. Gammon, D. Park, D. S. Katzer, and D. G. Steel, *Science* **282**, 1473 (1998).
- [30] P. Chen, C. Piermarocchi, and L. J. Sham, *Phys. Rev. Lett.* **87**, 67401 (2001).
- [31] T. Takagahara, *Phys. Stat. Sol.* **234**, 115 (2002).
- [32] V. Negoita, D. W. Snoke, and K. Eberl, *Phys. Rev. B* **60**, 2661 (1999).
- [33] A. Tackeuchi, T. Kuroda, K. Mase, Y. Nakata, and N. Yokoyama, *Phys. Rev. B* **62**, 1568 (2000).
- [34] C. Emary and L. Sham, *Phys. Rev. B* **75**, 125317 (2007).